Diffusion of Spheres in Entangled Polymer Solutions: A Return to Stokes–Einstein Behavior

Jongok Won,[†] Clement Onyenemezu,[‡] Wilmer G. Miller, and Timothy P. Lodge*

Department of Chemistry, University of Minnesota, Minneapolis, Minnesota 55455-0431

Received May 31, 1994; Revised Manuscript Received September 9, 1994[⊗]

ABSTRACT: Dynamic light scattering has been used to follow the tracer diffusion of polystyrene spheres ($R \approx 200$ nm) in dilute, semidilute, and entangled solutions of poly(vinyl methyl ether) ($M_w = 1.3 \times 10^6$). Over this range of matrix concentrations, $0 \le c[\eta] \le 36$, the diffusivity drops by almost 5 orders of magnitude. Near c^* ($\approx[\eta]^{-1}$) for the matrix, the diffusivity exceeds that estimated from the bulk solution viscosity via the Stokes–Einstein relation by a factor of about 3. Such "positive deviations" from Stokes–Einstein behavior have been reported previously in several systems. However, once the matrix concentration is sufficiently high for entanglements to be effective, Stokes–Einstein behavior is recovered. This new result was confirmed via forced Rayleigh scattering. In addition, these data can reconcile measurements of sphere diffusion with reptation-based models for chain mobility in well-entangled systems. The behavior near c^* is discussed in terms of the matrix correlation length, ξ, which has a maximum at $\xi \approx R_g$ for $c \approx c^*$. It is noted that the fluid layer within a distance ξ of the sphere surface will, in general, differ in composition from the bulk solution, and consequently the sphere mobility may well not sense the macroscopic solution viscosity, particularly near c^*. As a corollary, for large matrix chains, dynamic light scattering may not monitor the long-time diffusion of the spheres near c^*, because $q\xi \approx qR_g \approx 1$, rather than $q\xi \ll 1$.

Introduction

The tracer diffusion of spherical particles in polymer solutions has attracted a great deal of experimental attention.[1-24] The principal motivation has been to understand diffusion in solutions containing mixtures of macromolecules of differing architectures, which might serve, for example, to test modern treatments of polymer solution dynamics or as models of important biological systems. It is probably fair to say, however, that these goals have not been completely attained; the results in the literature diverge in interesting ways. Our own focus has been on the possible applicability of the reptation hypothesis, and we have previously reported extensive dynamic light scattering (DLS) measurements of the tracer diffusion of linear and star-branched polystyrenes (PS) in dilute, semidilute, and concentrated solutions of poly(vinyl methyl ether)s (PVME)[25,26] and also in PVME gels.[27,28] In this paper we describe results for the diffusion of PS spheres in some of the same PVME solutions. These new results display some novel features, relative to previous studies of sphere diffusion, yet are completely consistent with the qualitative picture that emerged from the linear and star PS diffusion. These results may help to reconcile some of the apparent contradictions among the earlier reports.

The diffusivity of a sphere is typically discussed in the context of the Stokes–Einstein (SE) relation:

$$D = \frac{kT}{6\pi\eta R} \qquad (1)$$

where R is the radius of the sphere and η is the zero-shear-rate viscosity of the medium in which it is suspended. This relation assumes that the medium may be treated as a continuum on the length scale of R, and the factor of 6π corresponds to a "stick" boundary condition at the sphere surface. Equation 1 works perfectly for noninteracting spheres in a small-molecule solvent, but it is certainly not obvious that an arbitrary polymer solution will satisfy the continuum assumption. For example, a polymer solution near its overlap concentration, c^*, will have a correlation length, ξ, on the order of the chain radius of gyration, R_g, which may easily be several tens of nanometers; this point has been amply recognized.[9] Consequently, the product $D\eta/D_0\eta_s$, where D_0 is the infinite dilution diffusivity of the sphere and η_s is the solvent viscosity, may deviate from unity as the polymer concentration increases. We will refer to $D\eta/D_0\eta_s > 1$ as a positive deviation from SE behavior and $D\eta/D_0\eta_s < 1$ as a negative deviation; a positive deviation corresponds to a diffusivity that decreases with increasing concentration less rapidly than the solution viscosity increases. Alternatively, one may use the measured diffusivity of a sphere of constant R to define a "microviscosity" or "effective viscosity" of the solution through eq 1. A positive deviation from SE behavior therefore corresponds to a microviscosity less than the macroscopic viscosity of the solution.

A complete review of the literature is beyond the scope of this paper, but the main results can be summarized as follows. Positive deviations,[7,11,12,21,23] negative deviations,[6,8,10,12,18] and adherence[1,8,13,14,16,18,22,24] to the SE relation have all been reported for various sphere/chain/solvent systems for measurements extending into the semidilute regime. In general, deviations are more common, and larger in magnitude, in ionic systems than in neutral solutions; in one polyelectrolyte matrix, a positive deviation in excess of 10^4 was reported.[11] It is also possible that the magnitude of the deviation is correlated with the stiffness of the matrix chains for a given matrix concentration. In organic solutions of flexible polymers, adherence to SE behavior is more common, but in one system a small positive deviation (less than a factor of 2),[23] and in another a small negative deviation,[29] have been noted. In both aqueous and organic solvents, negative deviations have, reason-

---

* To whom correspondence should be addressed.

[†] Current address: Korea Institute of Science and Technology, P.O. Box 131, Cheongryang, Seoul, Korea.

[‡] Current address: A. B. Dick & Co., Niles, IL 60648.

[⊗] Abstract published in *Advance ACS Abstracts,* October 15, 1994.

0024-9297/94/2227-7389$04.50/0

ably, been ascribed to chain adsorption and/or sphere aggregation, and we do not consider these further. Positive deviations can easily be justified when $R/\xi \ll 1$, i.e., for small spheres and large chains: the sphere can move through the solution without necessarily waiting for chains to relax their conformations. However, deviations have also been observed when $R/\xi > 1$.

As noted above, our measurements of linear and star PS diffusion in PVME solutions and gels have been aimed at assessing the applicability of the reptation hypothesis to solutions.[25-28] Our overall conclusions have been that (i) it is unlikely that reptation is the dominant mode of motion for linear chains in the semidilute regime (*i.e.*, $c^* \leq c \leq 0.10$ g/mL), primarily because it is difficult to achieve a sufficient number of entanglements per chain (*i.e.*, $M/M_e(c) > 5$, where M_e is the molecular weight between entanglements), but (ii) as c and M increase, a transition to reptation-like behavior is apparent. The latter conclusion is based, *inter alia*, on the progressive retardation of stars relative to linear chains of comparable size, the equivalence of linear chain mobility in solutions and gels for $c \approx 0.2$ g/mL, and molecular weight exponents for diffusion between -2 and -3, where -2 is the pure reptation limit and more negative values are ascribed to spatial randomness in the topological constraints. Of course, also underlying conclusion ii are the extensive data in polymer melts that support the reptation hypothesis,[30] combined with the expectation that solution behavior should approach melt behavior smoothly as c increases.

In contrast, Phillies has argued for the dominance of hydrodynamic interactions over topological (*i.e.*, entanglement) effects in solutions.[31] General adherence to the "stretched exponential" scaling relation

$$D = D_0 \exp(-\alpha c^u) \qquad (2)$$

for various tracers (linear and branched chains, globular proteins, hard spheres) in matrices of varying architecture (linear and branched chains, stiff chains, polyelectrolytes, *etc.*) in dilute and semidilute solutions has been noted[31,32] and advanced as an argument in favor of the dominance of hydrodynamics. Indeed, in at least one case eq 2 has been applied all the way up to the melt.[33] However, it was clear from our previous results for linear chains that eq 2 could not apply up to the melt in general, because extrapolation to $c = 1$ g/mL yielded implausible molecular weight exponents for D, *e.g.*, -6. In addition, the extensive measurements of polystyrene diffusion in concentrated solutions by Nemoto and coworkers[34,35] cannot be described by eq 2. More recently, Phillies has noted that a transition to meltlike behavior is seen in the viscosity at sufficiently high values of c and M and that the analog to eq 2 ceases to apply.[36] With this development, it becomes apparent that Phillies' overall conclusions are not necessarily inconsistent with our conclusions i and ii.

The remainder of this paper is organized as follows. After describing the experimental methodology, we present evidence that our PS spheres ($R \approx 200$ nm) are nearly monodisperse and do not aggregate in the PVME solutions considered here. These conclusions are based on static and dynamic light scattering and electron microscopy. Then, the diffusivity data (obtained via DLS) are presented and compared with the SE relation and with measurements of the same spheres diffusing in PS solutions. The PVME is of very high molecular weight (1.3×10^6), and the concentration range was such that $0 < c[\eta] < 36$; thus, the data extend significantly further into the entanglement regime than most of the systems studied previously. Concurrently, D/D_0 drops by nearly 5 orders of magnitude, which is approximately 2 orders of magnitude more than in any previous study. In selected solutions, forced Rayleigh scattering was used in conjunction with DLS to measure the sphere diffusion to establish that the long-time diffusion coefficient was determined in both techniques. Finally, the results are discussed, and the conclusions presented.

Experimental Section

Samples. Polystyrene (PS) latex spheres were prepared using 10 mol % divinylbenzene and 90 mol % styrene in an emulsifier-free emulsion polymerization as described elsewhere.[14,29] The sphere radius was determined to be 170 ± 10 nm by scanning electron microscopy, and the distribution of sphere sizes was narrow (*vide infra*). The poly(vinyl methyl ether) (PVME) sample used here is the same as that used previously in extensive studies of linear and star chain diffusion;[25,26] it has $M_w = 1.3 \times 10^6$ and a polydispersity less than 1.6. Spectrograde toluene (Aldrich) was used as the solvent, as it is a good solvent for both PS and PVME and nearly isorefractive with PVME ($dn/dc \approx 0.001$ mL/g). Ternary solutions were prepared by combining dilute, filtered binary sphere/toluene and PVME/toluene solutions. The sphere concentration was maintained very low (on the order of 10^{-5} g/mL) to prevent multiple scattering and to ensure that the measured diffusivity corresponded to the tracer diffusion of the spheres. As PVME is sensitive to oxidative degradation, a small amount (0.5% of the PVME concentration) of antioxidant, 4,4′-thiobis(*tert*-butyl-*m*-cresol) (Pfaltz and Bauer), was added to the PVME stock solution. For the dynamic light scattering measurements, the two stock solutions were mixed directly in a dust-free scattering cell and the solvent was evaporated off slowly, under flowing nitrogen, to achieve the desired PVME concentration. To prepare the four highest PVME concentrations, the PVME stock solution was centrifuged and only the upper portion was mixed with the sphere solution, without further filtration.

In order to attach to the spheres the photochromic moiety necessary for forced Rayleigh scattering (FRS), the PS latex was subjected to a three-step reaction, following the procedure outlined by Kim *et. al.*[37] The first reaction introduces phthalimidomethyl groups to the 4-position on the PS phenyl groups, randomly along the chain; these groups are transformed to aminomethyl groups in a second step. The dye, 4-(dimethylamino)azobenzene 4′-isothiocyanate (Pierce), referred to as DABITC, contains an isothiocyanate group which reacts with the aminomethyl group in the third phase of this sequence to yield the final product. The number of dye labels that were actually attached was determined by UV−vis spectrophotometry; the average ratio of the PS monomer per dye was found to be 25. Presumably, due to the limited degree to which solvent penetrates the spheres (*vide infra*), the labels are concentrated near the sphere surface. This labeling level is about an order of magnitude larger than that typically employed for FRS measurements of chain diffusion, but this was necessary due to the very small sphere concentrations in the final solutions. Even so, the net dye concentration in the FRS samples was approximately 2 orders of magnitude lower than in typical FRS measurements on polymer melts, which reduced the signal-to-noise ratio significantly.

Dynamic Light Scattering Measurements. Measurements were performed on a Malvern Model PCS-100 photogoniometer in combination with a Lexel 95−2 Ar$^+$ laser operated at 488 nm, a 264-channel multi-sample time correlator (Brookhaven Instruments BI-2030AT), and an ITT FW-130 photomultiplier tube. All measurements were taken at 30.0 ± 0.1 °C. For each solution, intensity correlation functions

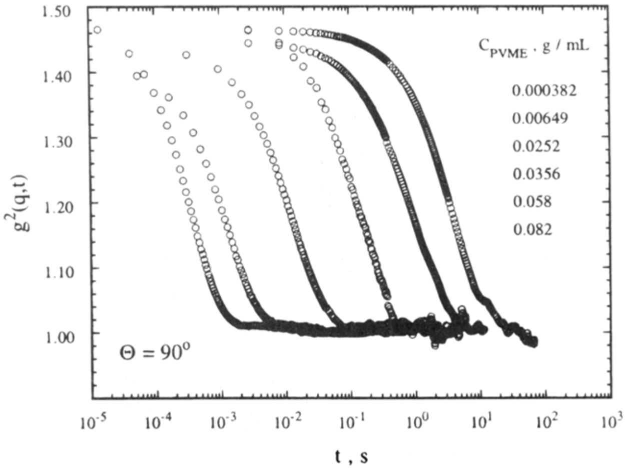

Figure 1. Intensity correlation functions for PS spheres in PVME solutions at a scattering angle of 90°. The curves correspond to the matrix concentrations indicated on the right side of the plot, with the concentrations increasing from left to right.

were accumulated at four or more scattering angles between 60 and 120°. Examples are shown in Figure 1, for a scattering angle of 90° and a wide range of matrix polymer concentrations. The decay rate, Γ, was extracted with a second-order cumulant fit. The diffusion coefficients were obtained by linear regression from plots of Γ versus q^2; the quality of the fit was good, and the intercept very close to zero, in all cases. The values of the normalized second cumulant for lower matrix concentrations were typically about 0.1 ± 0.02, but increased slightly (*i.e.*, to about 0.2 ± 0.06) with increasing concentration in the semidilute region. The majority of the correlation functions were also analyzed by the Laplace inversion routine CONTIN.[38] The resulting distribution of decay rates was dominated by a single peak, but in some cases a small-amplitude slow mode was resolved. Evidence of this slow decay can be seen in some of the correlation functions in Figure 1. The appearance/nonappearance of this slow peak was not simply correlated with matrix concentration, probe concentrations, or even scattering angle for a given solution, and so its exact origin is unclear. One possibility is number fluctuations, which can give rise to nonexponential slow decays. We estimate the typical number of particles in the scattering volume to be 10^3-10^4, so this effect should not be large. In any event, the mean decay rate associated with the dominant mode agreed very well with that from the cumulant analysis, with the CONTIN value of D systematically exceeding that from cumulant analysis by about 25%. Given the wide range of D values measured, this systematic difference is of no significance, and, for simplicity, we report here only the cumulant values. As the solutions were very viscous at high concentrations, sample homogeneity was checked by repeating the measurements until the value D no longer changed with time.

Forced Rayleigh Scattering Measurements. The FRS apparatus and experimental protocol have been described elsewhere.[39] Samples were prepared in 1 mm path length spectrophotometer cells and annealed in a bath at 30 °C for more than 4 months. The signal obtained in the experiment is the diffracted intensity decay due to diffusion of the dye-labeled spheres. The diffraction grating was generated using 100 mW of 488 nm light from an Ar^+ laser and a pulse width of 10 ms. The decay was monitored using an attenuated (*i.e.*, $\times 10^{-4}$) beam from the same laser. The FRS decays were fit to the following functional form:

$$I(t) = [A \exp(-t/\tau) + B]^2 + C^2 \tag{3}$$

where $I(t)$ is the measured intensity, τ is the time constant for the decay, and A, B, and C are proportional to the amplitudes of the diffracted, coherently scattered, and incoherently scattered electric fields, respectively. In this system, the thermal reisomerization of the dye occurs on the same time scale as diffusion, such that

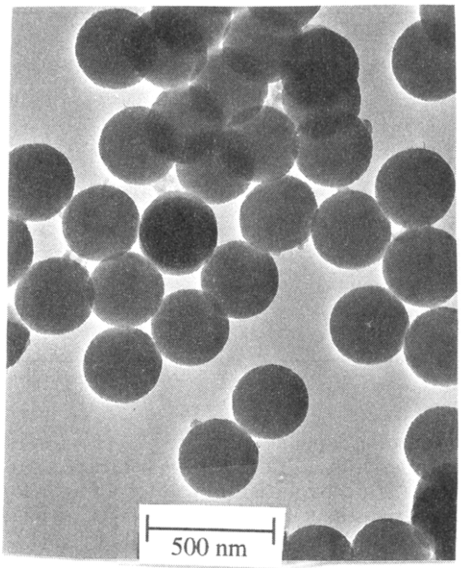

Figure 2. Transmission electron micrograph of the dye-labeled PS spheres at a magnification of 42 000.

$$\frac{1}{\tau} = \frac{1}{\tau_1} + \frac{4\pi^2 D}{d^2} \tag{4}$$

where τ_1 is the dye lifetime and d is the grating spacing. Measurements were made at several grating spacings, and D was extracted from a (linear) plot of $1/\tau$ versus $1/d^2$. FRS measurements were also made for several different positions in each cell, until the various values of τ agreed to within 40%. All measurements were made at 30.0 ± 0.2 °C.

Transmission Electron Microscopy. The size of the DABITC-labeled latex was investigated by transmission electron microscopy (TEM) to ensure that the reaction procedure had no gross effect on the spheres. The labeled latex was dispersed in toluene (*ca.* 0.5 vol %) and mounted on a carbon-coated TEM grid. The solvent was evaporated off at room temperature, and the electron micrograph was obtained with a Philips CM-30 TEM; a typical image, with a magnification of 42 000, is shown in Figure 2. The results suggest that the dye-labeled spheres were not perturbed by the reaction procedure.

Attempts were also made to use TEM to ascertain the state of dispersion of the spheres in concentrated PVME solutions; of particular interest is the possibility of sphere aggregation. To prepare a solution for TEM observation, drops of the samples were mounted in a gold specimen holder and then rapidly vitrified by immersion in a bath of liquid propane surrounded by liquid nitrogen. The specimen was then fractured under vacuum (2×10^{-6} Torr) at −120 °C in a freeze−etch apparatus (Balzers). The fracture surface was replicated with a platinum−carbon mixture. The sample and replica were removed from the vacuum chamber, and the sample was dissolved in a toluene bath at room temperature, leaving the platinum−carbon replica behind. The replicas were washed in distilled water and collected on electron microscopy grids. The replicas were then examined in the Philips CM-30 microscope in the conventional transmission mode.

Results

Sphere Size and Structure. The form factor for a hard sphere is given by

$$P(q) = 9(qR)^{-6}(\sin qR - qR \cos qR)^2 \tag{5}$$

The angular dependence of the excess scattered inten-

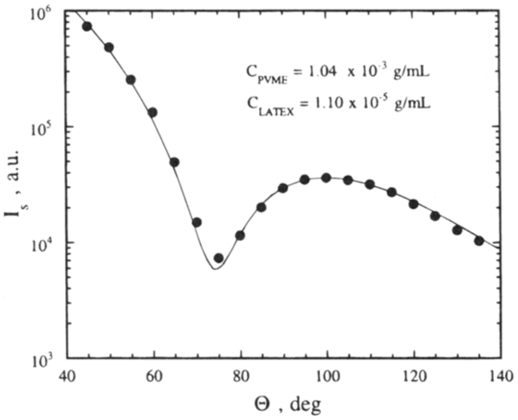

Figure 3. Angular dependence of the excess scattered intensity for PS spheres in a dilute PVME solution. The smooth curve represents a convolution of the form factor for a hard sphere with a Gaussian distribution of sphere sizes with a polydispersity of 5%.

sity for a solution with a PVME concentration of 1.04 × 10^{-3} g/mL and a sphere concentration of 1.15 × 10^{-5} g/mL is shown in Figure 3; a pronounced minimum is apparent near a scattering angle of $\theta = 74°$. The smooth curve represents a convolution of eq 5 with a Gaussian distribution of sphere sizes, following the approach of Cumming *et al.*[40] The curve describes the data extremely well, with a mean radius of 194 nm and a polydispersity of about 5%; due to finite instrument resolution, the actual polydispersity is probably somewhat less. DLS measurements on binary sphere/toluene solutions yielded a value for the hydrodynamic radius (equal to the hard sphere radius) of 197 ± 5 nm, in excellent agreement with the result from Figure 3. These values are only slightly larger than that estimated from electron microscopy, indicating that these highly cross-linked spheres are swollen to a rather small extent, even in toluene, a good solvent for polystyrene. A similar conclusion was presented previously, where R = 209 ± 5 nm was determined by DLS in another good solvent, dimethylformamide.[14] We repeated measurements of the angle dependence of the excess scattered intensity for sphere concentrations ranging from 6.5 × 10^{-6} to 4.8 × 10^{-5} g/mL and in solutions with matrix concentrations both above and below c^*, with no significant changes noted. This range of sphere concentrations brackets those used in the diffusion measurements and confirms that there is no multiple scattering over this concentration range.

To interpret the diffusion results correctly, it is important to establish the structure of the sphere dispersion, *e.g.*, whether or not there is substantial aggregation or association of the spheres. As noted in the Introduction and discussed elsewhere,[14] this issue has cast some doubt on the interpretation of previous measurements of sphere diffusion. In our measurements, aggregation is of most concern at higher matrix concentrations, where the diffusion results are the most interesting. The following evidence argues against substantial association of the spheres. First, the angular dependence of the excess scattered intensity was measured as a function of matrix concentration, up to 5.9 × 10^{-2} g/mL, with no significant changes observed. In particular, the distinct minimum near θ = 74° persists. This observation also demonstrates that there is no change with matrix concentration in either the amount or the radial distribution of solvent molecules imbibed by the spheres. Second, no substantial increases in scattered intensity with matrix concentration were observed. Third, the freeze–fracture TEM pictures do not suggest significant aggregation; an example is shown in Figure 4 for a matrix concentration of 1.40 × 10^{-2} g/mL, which is just into the entangled regime (*vide infra*). The TEM sample preparation procedure should not alter the structure of the solution significantly, as the system becomes glassy on the millisecond time scale. In this micrograph, only dispersed spheres appear. The variation in apparent sphere size reflects the exposure of the spheres across the fracture surface. Fourth, the modest increase in the normalized second cumulant, k_2, with increasing matrix concentration could indicate some association of the spheres, but not an extensive effect. Following the analysis of Bargeron,[41] a doubling of k_2 signifies a doubling in the width of the size distribution, *i.e.*, from about 5% to about 10%, based on the polydispersity obtained from Figure 3, or from about 10% to 20%, based on the k_2 values themselves. The values of k_2 can also be enhanced by the slow decay discussed in the Experimental Section. An additional possible contribution to the increase in k_2 could be a distribution of mobilities that arises naturally near c^*, due to matrix concentration fluctuations and the length scale of the measurement. The latter possibility will be discussed subsequently, but it is worth noting that a comparable increase in k_2 has been reported for the tracer diffusion of polystyrene[37] and poly(methyl methacrylate)[42] chains in semidilute solutions, measured by FRS.

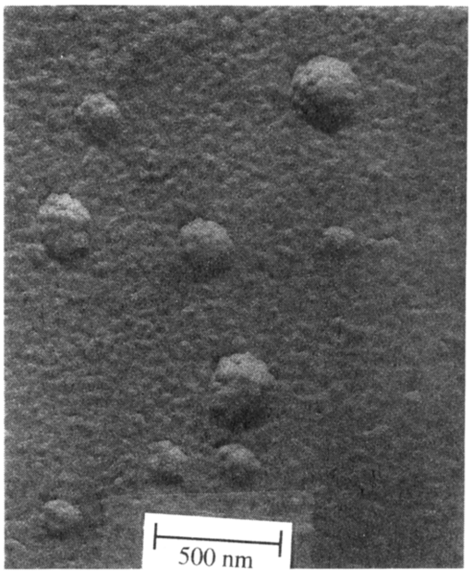

Figure 4. Transmission electron micrograph of a freeze–fracture replica of an entangled sphere/polymer solution at a magnification of 42 000.

Sphere Diffusion. The DLS diffusion data are presented as a function of matrix concentration in Figure 5 in a double-logarithmic format. By the highest matrix concentration, the mobility of the spheres has decreased by well over 4 orders of magnitude; as far as we are aware, the largest drop reported previously has been less than 3 orders of magnitude. Significant decreases in mobility do not begin to appear until a matrix concentration of 0.006 g/mL. The size of the individual symbols corresponds to an uncertainty of ±15%, which is consistent with the typical uncertainties from the plots of Γ vs q^2. However, inspection of the entire data set in Figure 5 suggest that there may be somewhat larger, random errors. For example, near c = 0.006 g/mL the diffusivity appears to drop abruptly

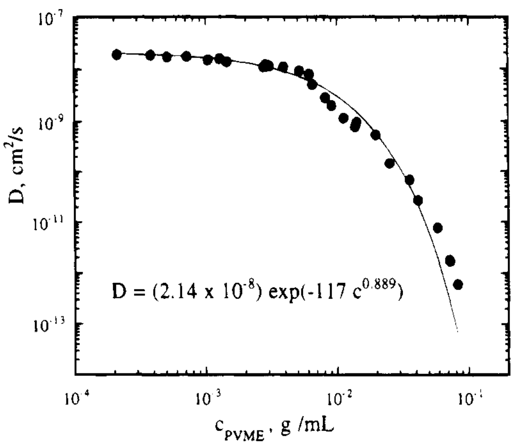

Figure 5. Tracer diffusion coefficient of PS spheres in PVME solutions as a function of matrix concentration. The smooth curve represents the equation shown on the plot.

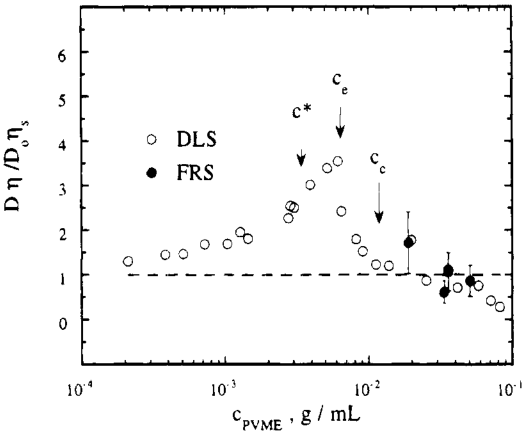

Figure 6. Product of the sphere diffusivity and the solution viscosity normalized by the corresponding values at infinite dilution as a function of matrix concentration. The dashed line corresponds to the Stokes–Einstein relation.

by a factor of 2, which would be unusual. A fit of the data of eq 2 by nonlinear regression is also shown in figure, with D_0 fixed at the measured value of 2.14×10^{-8} cm²/s. Equation 2 does not describe the data very well, in the sense that the residuals are not randomly distributed about zero as a function of the independent variable and because the fit deviates from the data by about an order of magnitude at the highest concentration examined. The data were also fit to the same functional form, but as $\ln(D/D_0)$ vs $-\alpha c^u$, which is tantamount to assuming that the relative error in D is independent of c. The resulting parameter values are different—*i.e.*, α changes from 117 to 163.5 and u from 0.889 to 1.004—but the resulting curve itself is similar to that shown in Figure 5.

The zero-shear-rate viscosity, η, for this PVME in *o*-fluorotoluene was measured previously as a function of concentration up to $c = 0.20$ g/mL.[26] Thus it is possible to assess whether these spheres exhibit Stokes–Einstein (SE) behavior over some range of concentration. Accordingly, in Figure 6 the product $D\eta/D_0\eta_s$ is plotted against c, where η_s is the solvent viscosity and D_0 is the infinite dilution diffusion coefficient. The values of η were interpolated to the exact concentrations used for the diffusivity measurements using a stretched exponential function, and the difference between the two solvents was ignored (the viscosities of toluene and *o*-fluorotoluene are very similar). SE behavior would correspond to a constant value of unity for this product, which is indicated by the horizontal dashed line. The results are remarkable. At low matrix concentrations, $D\eta/D_0\eta_s$ increases with increasing c, up to a maximum value between 3 and 4. However, above a matrix concentration of 0.006 g/mL, $D\eta/D_0\eta_s$ decreases quite sharply, and SE behavior is recovered. As far as we are aware, this is the first time such a return to SE behavior, after an initial positive departure, has been seen. (Ullmann *et al.*[20] noted a sphere diffusivity that initially *increased* by about 50% with increasing matrix concentration, followed by a decrease when $c > 0.01$ g/mL, but as the matrix molecular weight was reported to be 1.85×10^4, this is unlikely to be correlated with entanglements. Furthermore, our diffusivities are monotonically decreasing functions of matrix concentration, so we are hesitant to ascribe a common origin to our observations and those of Ullmann *et al.*) For the two highest concentrations, $D\eta/D_0\eta_s$ appears to drop below unity, but it is not clear to what extent this reflects uncertainties in the measurements of D and η. For example, $D \approx 10^{-12}$ cm²/s at these concentrations, which is approaching the practical lower limit for DLS. Furthermore, the viscosity measurements for $c > 0.04$ g/mL were made in a commercial rheometer which could not be sealed to the atmosphere, and so solvent-saturated sponges were placed around the sample; the possibility of a small amount of solvent evaporation or condensation cannot be discounted, which becomes especially important where $\partial\eta/\partial c$ is largest, *i.e.*, at large c.

Three particular concentrations are denoted in Figure 6. The coil overlap concentration, c^*, was estimated to be 0.0033 g/mL, as $1.5/[\eta]$; this definition of c^* is roughly equivalent to $3M/N_a(4\pi R_g^3)$ via the Flory–Fox relation. The entanglement concentration, c_e, was estimated on the basis of $M_e°$, the melt value for the molecular weight between entanglements. The critical concentration, c_c, was estimated from a plot of η vs c and is comparable to $2c_e$, consistent with the rule of thumb that $2M_e° \approx M_c°$ in the melt. Clearly, there is always some arbitrariness in the definition of any of these concentrations, but the important points here are that (i) the maximum deviation from SE behavior occurs near c^*, where ξ is greatest, and (ii) the return to SE behavior coincides with the onset of entanglements.

Discussion

Prior to discussing the behavior illustrated in Figure 6, there are two related issues on which we would like to comment. These are (i) to what extent should spheres be viewed as "probes" in polymer solutions and (ii) does DLS measure the long-time diffusion of large spheres?

Spheres as Probes. Any species present in vanishing amount in a polymer solution can, in some sense, be considered a "probe", with the expectation that the measured behavior of the probe can yield useful information about the properties of the system. However, the tacit assumption is that the probe has no significant influence on the matrix. For the specific case of a hard sphere dispersed in a solution of flexible polymers, it seems to us that this assumption cannot hold. When a labeled flexible chain or small molecule is added to the solution, one can view the probe as replacing a matrix chain or solvent molecule, respectively, with negligible effect on the solution in the immediate vicinity of the probe. In contrast, a hard sphere cannot "replace" a matrix chain in a literal sense; rather, it displaces a substantial volume of solution and replaces it with a rigid object. For example, each of our spheres would effectively displace 2000 PVME chains when $c = 0.1$

g/mL. Furthermore, the structure, and presumably the dynamics, of the solution is perturbed over a significant distance away from the sphere surface. For example, in the case of a dilute solution near a noninteracting surface, it is anticipated that there is a depletion zone extending a distance $\approx R_g$ in the solution;[43] R_g for this PVME sample is estimated to be 54 nm, which is a significant fraction of the sphere radius. In the semidilute regime, the extent of the depletion zone decreases with the solution correlation length, ξ, but can still be significant. If the surface–chain interaction is attractive, there is a concentration enhancement within a layer of width ξ adjacent to the surface. In any circumstance (*i.e.*, attractive, repulsive, or neutral sphere–chain interactions), the properties of the fluid in the vicinity of the sphere may differ markedly from those of the bulk, and the diffusion of the sphere over distances comparable to ξ will not necessarily "probe" the bulk solution properties. Thus, we feel that use of the term "probe" in reference to spheres in polymer solutions can be misleading.

Long-Time Diffusion. DLS follows the dynamics of concentration fluctuations, and often the observed behavior is diffusive ($\Gamma \sim q^2$). However, to determine the tracer diffusion of a polymer or particle, at least two conditions should be met. First, the scattering particle should be present in sufficiently low concentration that the observed mutual diffusion coefficient approaches the translational diffusion coefficient of the particle. This is clearly the case herein. Second, the quantity qR, where R is the polymer or particle size, should be much less than unity. This second condition effectively requires that the tracer move many times its own radius during the time scale of the measurement. In our measurements, $3.9 < qR < 7.7$, so one may well ask how we can measure long-time diffusion at all. The answer is that a rigid particle has no internal modes, so that only diffusion contributes to motion on any length scale. However, there is a third requirement: $q\xi$ should be much less than unity. This condition simply indicates that the particle motions average over the properties of the bulk fluid. In a small-molecule solvent the matrix "correlation length" is less than 1 nm and thus in dilute solution one may be confident that long-time diffusion can be measured. Certainly, the exact agreement obtained between the mean sphere radius determined from the angular dependence of the scattered intensity and that obtained from the infinite dilution diffusivity (via the SE relation) confirms this. However, in a polymer solution near c^*, $\xi \approx R_g$, and it is not at all clear that DLS will necessarily measure long-time diffusion. In our measurements, $1 \le q\xi \le 2$ near c^*. Given that we expect the PS–PVME interaction to be effectively neutral, there should be a depletion zone around the sphere, and consequently for motion on the length scale of ξ, this could contribute to a positive deviation from SE behavior.

To address this issue, we undertook FRS measurements of sphere diffusion at selected concentrations, because the diffusion distance in FRS is 1–2 orders of magnitude larger than in DLS. In Figure 6, the four solid symbols denote the FRS measurements. Clearly, in this concentration range the FRS and DLS data agree perfectly, confirming that DLS is monitoring long-time diffusion. Unfortunately, signal quality prevented accurate FRS measurements at lower matrix concentrations, so it was not possible to assess whether the agreement between FRS and DLS persisted near c^*. However, the FRS results confirm (i) that the return to SE behavior is real, (ii) that number fluctuations play no significant role in the determination of D, and (iii) that the detailed chemistry of the sphere surface plays little role in transport, given that the labeled spheres have many photochromic dyes on or near the surface.

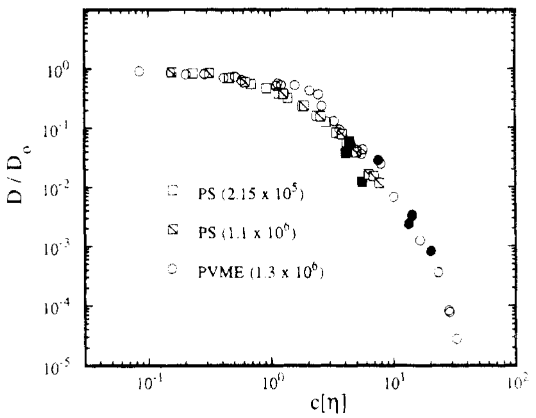

Figure 7. Reduced sphere diffusivity versus reduced matrix concentration for PS spheres in PS/DMF and PVME/toluene solutions. The filled symbols correspond to measurements made by forced Rayleigh scattering.

Comparison with Other Sphere/Polymer Systems. As noted previously, this is the first time that a return to SE behavior has been reported after an initial significant departure. Recently, Onyenemezu *et al.* examined the diffusion of the same spheres in a matrix of PS chains in DMF, a good solvent, also by DLS.[14] They found complete adherence to the SE relation for two different matrix molecular weights. A comparison of their data with those in Figure 5 is presented in Figure 7. Here, the concentration axis is normalized by $[\eta]$ for the matrix. In addition, we have made FRS measurements of the spheres in some PS/DMF solutions, and these points are also included as the solid symbols. The superposition is quite good, particularly at low and high concentrations. The deviation from SE behavior in the PVME system appears as a breakdown of superposition near $c[\eta] = 2$, or $c \approx c^*$. However, it is interesting to note that in this plotting format, the departure from SE behavior, while distinct, is rather inconsequential in the overall picture. The FRS measurements in the PS/DMF solutions also confirm that the long-time diffusion was measured by DLS.[14]

We have no clear understanding of why the SE relation is followed in the PS solutions but not always in the PVME matrices. For the PVME system, the return to SE behavior at $c \approx c_e$ is intuitively very reasonable; it indicates that in a dynamic sense the matrix appears as a continuum to the spheres. In other words, the motion of the spheres is now limited by the relaxation of matrix entanglements. Similarly, near c^*, the spatial inhomogeneity of the solution concentration is greatest, and the motion of the spheres is not completely coupled with the chain relaxation. The difficulty with this interpretation is that in the PS matrix the maximum value of ξ (estimated as R_g) is only about 30% lower than in the PVME case, yet the SE is still followed. Interestingly, unpublished results for the diffusion of the same spheres in poly(vinylpyrrolidone)/water solutions have observed a departure from SE behavior, by a factor of about 3, followed by a return at higher matrix concentrations.[29]

The superposition of the data in the two different matrix polymers in Figure 7 is strong evidence that

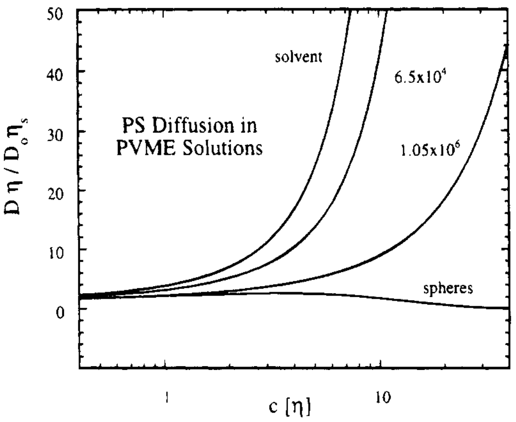

Figure 8. Comparison of the concentration dependence of diffusion for solvent,[26] linear polystyrenes with $M = 6.5 \times 10^4$ and 1.05×10^6,[26] and PS spheres in PVME solutions; the actual data have been replaced by smooth curves representing fits to eq 2.

there are no specific sphere–polymer interactions of significance. In the PS case, there is no reason to anticipate any unusual interactions, because the spheres and the chains are chemically very similar and the solvent is good. Furthermore, studies with labeled polystyrene chains indicate no significant adsorption of chains onto the spheres in good solvents.[44] In the PVME case, one might be concerned about chains adsorbing to the spheres, given that the PS/PVME interaction parameter is slightly negative. However, the fact that the spheres are, if anything, more mobile in PVME solutions than in PS solutions argues against this. It should also be recalled that in our previous studies we found no unusual interactions between PS and PVME chains up to matrix concentrations as high as 0.3 g/mL.[25,26] Finally, we feel it is unlikely that the matrix chains penetrate the spheres, given the limited extent to which good solvents swell the spheres. The point to be underscored, therefore, is that the return to SE behavior in Figure 6 is clearly not an artifact associated with this particular chemical system.

Two other reports of spheres diffusing in organic systems have appeared. Brown and Zhou showed that stearic acid coated silica spheres followed SE behavior in polyisobutylene (PIB)/$CHCl_3$ solutions[3,22] but exhibited a small positive deviation (by a factor of about 1.5) in poly(ethylene oxide)/CH_3OH solutions.[23] The maximum matrix concentrations were $c[\eta] \approx 3$ in these studies, and a return to SE behavior was not seen in the latter case. In both systems, plots of D/D_0 vs c/c^* superposed well, and so our data appear to be broadly consistent with theirs.

Comparison with Flexible Chain Diffusion. As mentioned in the Introduction, we have made extensive measurements of PS chain diffusion in the same PVME matrix,[25,26] and there remains some controversy about what one learns from comparisons of sphere and chain diffusion.[4,17] In Figure 8, we compare the diffusion of solvent (in this case, *o*-fluorotoluene[25,26]), a low-*M* PS chain, a high-*M* PS chain, and the PS spheres in the format of Figure 6, *i.e.*, highlighting departures from SE behavior. For simplicity, the individual data sets, including the viscosity, have been represented as smooth curves via fits to eq 2. (Note that even solvent diffusion follows eq 2 very well.) There are several important conclusions that may be drawn from this figure. First, the curves are monotonic in diffusant size. The solvent is the most mobile, and the spheres the least. Second, whereas the difference between the curves for the larger linear polymer and the sphere is discernible at $c[\eta] \approx 2$, substantial differences do not appear until $c[\eta] \approx 5-6$, which is consistent with the onset of entanglement effects as seen in the matrix viscosity. Third, for chains the departure of $D\eta/D_0\eta_s$ from 1 is concave up. This is qualitatively in agreement with the reptation model, in which viscosity increases more rapidly with number of entanglements per chain than the diffusivity decreases. In contrast, the sphere diffusion goes through a maximum before decreasing. (Note that the sphere curve in Figure 8 goes to zero at high c. This is an artifact of the use of eq 2, which does not fit either D or η perfectly; the product of two different stretched exponentials will always tend to very small or very large numbers, as c increases.)

As a consequence of the results in Figure 8, combined with the previous discussion of spheres as "probes", we wonder when it may be appropriate to use measurements of sphere diffusion to draw conclusions about the mechanism of diffusion for flexible chains. For example, Phillies, Brown, and Zhou presented a comparison of silica sphere and PIB chain diffusion in PIB solutions for tracers of comparable radius and found the spheres to be more mobile.[17] They concluded that under "conditions optimal for observing the diffusion of reptational behavior" their data "conclusively reject...reptational models for polymers dynamics". However, their data were obtained only up to matrix concentrations corresponding to $c[\eta] < 6$ for the spheres and $c[\eta] < 2$ for the chains, clearly insufficient to investigate entangled solution dynamics. (Phillies *et al.*[17] estimated c_e for the PIB solutions using $M_e°$ from the melt but arrived at a value of $c_e < 1/[\eta]$, which seems unrealistic; the difficulty of estimating c_e from M_e^0 for high molecular weight chains was noted by Ferry.[45])

Conclusion

We have used dynamic light scattering to follow the tracer diffusion of PS spheres ($R \approx 200$ nm) in dilute, semidilute, and entangled solutions of PVME chains ($M_w = 1.3 \times 10^6$). Over the range of matrix concentrations examined ($0 \le c[\eta] \le 36$) the diffusivity drops by almost 5 orders of magnitude. Using previously measured solution viscosities, the data were compared with the Stokes–Einstein (SE) relation. The principal new result of this work is that although a positive deviation from SE behavior is observed near c^* for the matrix, SE behavior is recovered once the matrix becomes sufficiently entangled. Possibly, previous studies of sphere diffusion were not extended to sufficiently high concentration (*i.e.*, $c \gg c^*$ and $R \gg \xi$) to observe this phenomenon.

A quantitative explanation for the positive deviation from SE is not yet available, but it is probably correlated with the fact that the matrix correlation length, ξ, has a maximum near c^*. An interesting aspect of the problem is that the fluid within a distance ξ of the sphere surface may have different composition from the bulk, and this could certainly influence sphere diffusion over this length scale. For our system, in which the surface–matrix interaction is assumed to be neutral, a depletion layer would exist, leading to an enhanced short-time diffusion for the spheres. As a corollary, for large matrix chains such as those employed here, DLS may not measure the long-time diffusion of the spheres if $q\xi \approx 1$. Forced Rayleigh scattering was employed to assess this possibility, but signal limitations prevented reliable measurements near c^*. Measurements were possible at higher c, however, and confirmed that in this region DLS did measure long-time diffusion. Finally, the results presented herein are completely consistent with our previous studies of PS chain diffusion in PVME solutions, in which we concluded that at sufficiently high matrix molecular weights and concentrations, a transition to reptation-like (or melt-like) diffusion occurs.

Acknowledgment. This work was supported by a grant from the Petroleum Research Fund, administered by the American Chemical Society (T.P.L.), and by an Exxon Education Foundation Grant from Research Corporation (C.O.). The assistance of Mr. Shin with the TEM measurements is appreciated.

References and Notes

(1) Brown, W.; Rymden, R. *Macromolecules* **1988**, *21*, 840.
(2) Brown, W.; Rymden, R. *Macromolecules* **1986**, *19*, 2942.
(3) Brown, W.; Zhou, P. *Macromolecules* **1989**, *22*, 4031.
(4) Brown, W.; Zhou, P. *Polymer* **1990**, *31*, 772.
(5) Brown, W.; Rymden, R. *Macromolecules* **1987**, *20*, 2867.
(6) Cooper, E. C.; Johnson, P.; Donald, A. M. *Polymer* **1991**, *32*, 2815.
(7) Furukawa, R.; Arauz-Lara, J. L.; Ware, B. R. *Macromolecules* **1991**, *24*, 599.
(8) Gorti, S.; Ware, B. R. *J. Chem. Phys.* **1985**, *83*, 6449.
(9) Langevin, D.; Rondelez, F. *Polymer* **1978**, *19*, 875.
(10) Lin, T.-H.; Phillies, G. D. J. *J. Phys. Chem.* **1982**, *86*, 4073.
(11) Lin, T.-H.; Phillies, G. D. J. *J. Colloid Interface Sci.* **1984**, *100*, 82.
(12) Lin, T.-H.; Phillies, G. D. J. *Macromolecules* **1984**, *17*, 1686.
(13) Nehme, O. A.; Johnson, P.; Donald, A. M. *Macromolecules* **1989**, *22*, 4326.
(14) Onyenemezu, C. N.; Gold, D.; Roman, M.; Miller, W. G. *Macromolecules* **1993**, *26*, 3833.
(15) Phillies, G. D. J.; Malone, C.; Ullmann, K.; Ullmann, G. S.; Rollings, J.; Yu, L.-P. *Macromolecules* **1987**, *20*, 2280.
(16) Phillies, G. D. J.; Gong, J.; Li, L.; Rau, A.; Zhang, K.; Yu, L.-P.; Rollings, J. *J. Phys. Chem.* **1989**, *93*, 6219.
(17) Philies, G. D. J.; Brown, W.; Zhou, P. *Macromolecules* **1992**, *25*, 4948.
(18) Russo, P. S.; Mustafa, M.; Cao, T.; Stephens, L. K. *J. Colloid Interface Sci.* **1988**, *122*, 120.
(19) Ullmann, G.; Phillies, G. D. J. *Macromolecules* **1983**, *16*, 1947.
(20) Ullmann, G. S.; Ullmann, K.; Lindner, R. M.; Phillies, G. D. J. *J. Phys. Chem.* **1985**, *89*, 692.
(21) Yang, T.; Jamieson, A. M. *J. Colloid Interface Sci.* **1988**, *126*, 220.
(22) Zhou, P.; Brown, W. *Macromolecules* **1989**, *22*, 890.
(23) Zhou, P.; Brown, W. *Macromolecules* **1990**, *23*, 1131.
(24) Tracy, M. A.; Pecora, R. *Macromolecules* **1992**, *25*, 337.
(25) Lodge, T. P.; Markland, P.; Wheeler, L. M. *Macromolecules* **1989**, *22*, 3409.
(26) Wheeler, L. M.; Lodge, T. P. *Macromolecules* **1989**, *22*, 3399.
(27) Rotstein, N. A.; Lodge, T. P. *Macromolecules* **1992**, *25*, 1316.
(28) Won, J.; Lodge, T. P. *J. Polym. Sci., Polym. Phys. Ed.* **1993**, *31*, 1897.
(29) Onyenemezu, C. Ph.D. Thesis, University of Minnesota, 1994.
(30) Lodge, T. P.; Rotstein, N. A.; Prager, S. *Adv. Chem. Phys.* **1990**, *79*, 1.
(31) Phillies, G. D. J. *J. Phys. Chem.* **1989**, *93*, 5029.
(32) Phillies, G. D. J.; Peczak, P. *Macromolecules* **1988**, *21*, 214.
(33) Phillies, G. D. J. *Macromolecules* **1986**, *19*, 2367.
(34) Nemoto, K.; Kishine, M.; Inoue, T.; Osaki, K. *Macromolecules* **1990**, *23*, 659.
(35) Nemoto, N.; Kojima, T.; Inoue, T.; Kishine, M.; Hirayama, T.; Kurata, M. *Macromolecules* **1989**, *22*, 3793.
(36) Phillies, G. D. J. *J. Phys. Chem.* **1992**, *96*, 10061.
(37) Kim, H.; Chang, T.; Yohanan, J. M.; Wang, L.; Yu, H. *Macromolecules* **1986**, *19*, 2737.
(38) Provencher, S. W. *Comput. Phys. Commun.* **1982**, *27*, 229.
(39) Huang, W. J.; Frick, T. S.; Landry, M. R.; Lee, J. A.; Lodge, T. P.; Tirrell, M. *AIChE J.* **1987**, *33*, 573.
(40) Cumming, A.; Wiltzius, P.; Bates, F. S.; Rosedale, J. H. *Phys. Rev. A* **1992**, *45*, 885.
(41) Bargeron, C. B. *J. Chem. Phys.* **1974**, *61*, 2134.
(42) Faldi, A.; Tirrell, M.; Lodge, T. P. *Macromolecules* **1994**, *27*, 4176.
(43) de Gennes, P.-G. *Scaling Concepts in Polymer Physics*; Cornell University Press: Ithaca, NY, 1979.
(44) Fedie, R. L.; Miller, W. G. *Polym. Mater. Sci. Eng.* **1994**, *71*, 344.
(45) Ferry, J. D. *Viscoelastic Properties of Polymers*, 3rd ed.; Wiley: New York, 1980.